

## Fugitive Road Dust PM<sub>2.5</sub> Emissions and Their Potential Health Impacts

Siyu Chen,<sup>†</sup> Xiaorui Zhang,<sup>†</sup> Jintai Lin,<sup>‡</sup> Jianping Huang,<sup>\*,†</sup> Dan Zhao,<sup>†</sup> Tiangang Yuan,<sup>†</sup> Kangning Huang,<sup>§</sup> Yuan Luo,<sup>†</sup> Zhuo Jia,<sup>||</sup> Zhou Zang,<sup>†</sup> Yue'an Qiu,<sup>⊥</sup> and Li Xie<sup>#</sup>

<sup>†</sup>Key Laboratory for Semi-Arid Climate Change of the Ministry of Education, Lanzhou University, Lanzhou 730000, P. R. China

<sup>‡</sup>Laboratory for Climate and Ocean-Atmosphere Studies, Department of Atmospheric and Oceanic Sciences, School of Physics, Peking University, Beijing 100871, P. R. China

<sup>§</sup>Yale School of Forestry and Environmental Studies, Yale University, New Haven, Connecticut 06511, United States

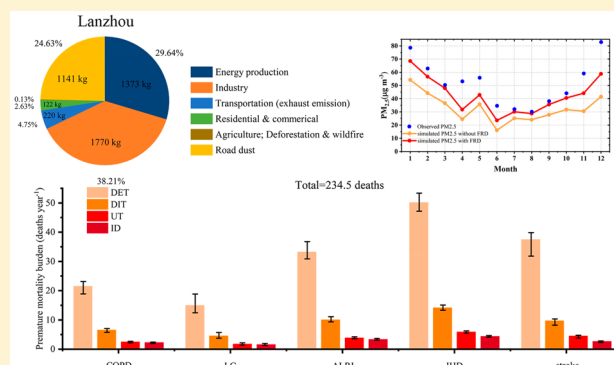
<sup>||</sup>College of Earth and Environmental Sciences, Lanzhou University, Lanzhou 730000, P. R. China

<sup>⊥</sup>School of Geography and Planning, and Guangdong Key Laboratory for Urbanization and Geo-Simulation, Sun Yat-sen University, Guangzhou 510275, P. R. China

<sup>#</sup>Gansu Provincial Maternity and Child Care Hospital, Lanzhou 730050, P. R. China

### Supporting Information

**ABSTRACT:** Fugitive road dust (FRD) particles emitted by traffic-generated turbulence are an important contributor to urban ambient fine particulate matter (PM<sub>2.5</sub>). Especially in urban areas of developing countries, FRD PM<sub>2.5</sub> emissions are a serious environmental threat to air quality and public health. FRD PM<sub>2.5</sub> emissions have been neglected or substantially underestimated in previous study, resulting in the underestimation of modeling PM concentrations and estimating their health impacts. This study constructed the FRD PM<sub>2.5</sub> emissions inventory in a major inland city in China (Lanzhou) in 2017 at high-resolution (500 × 500 m<sup>2</sup>), investigated the spatiotemporal characteristics of the FRD emissions in different urban function zones, and quantified their health impacts. The FRD PM<sub>2.5</sub> emission was approximately 1141 ± 71 kg d<sup>-1</sup>, accounting for 24.6% of total PM<sub>2.5</sub> emission in urban Lanzhou. Spatially, high emissions exceeding 3 × 10<sup>4</sup> μg m<sup>-2</sup> d<sup>-1</sup> occurred over areas with smaller particle sizes, larger traffic intensities, and more frequent construction activities. The estimated premature mortality burden induced by FRD PM<sub>2.5</sub> exposure was 234.5 deaths in Lanzhou in 2017. Reducing FRD emissions are an important step forward to protect public health in many developing urban regions.



### INTRODUCTION

Particulate matter (PM), a major environmental threat around the world, plays an important role in ambient air quality degradation as well as in acute damage to public health.<sup>1–4</sup> Fugitive road dust (FRD) particles are those emitted from roads into the ambient atmosphere by traffic-generated turbulence.<sup>5–7</sup> Sources of these particles include surrounding soils, mud carried by vehicles, demolition and construction, fly ash from asphalt, bioclastics, natural dust deposition, and other processes.<sup>8,9</sup>

Over the recent decades, the contribution of FRD to the total PM has become increasingly important due in part to rapid growth of the global number of vehicles worldwide, i.e., approximately 4% per year from 2006 to 2013.<sup>7,10</sup> This contribution is especially prominent in China, where the vehicle number has increased at a rate of 15% per year from 2015 to 2018.<sup>10–14</sup> Global measurements indicated that FRD emissions accounted for 55% of the PM<sub>10</sub> (particles with

aerodynamic diameter < 10 μm) concentrations in Delhi, India, in 2010,<sup>15</sup> 25.7% of PM<sub>10</sub> in Brazil, São Paulo, in 2014,<sup>16</sup> and 14–48% of PM<sub>10</sub> in European urban areas from 2000 to 2009.<sup>17</sup>

FRD particles are an important carrier for high levels of harmful components such as heavy metal elements (i.e., Pb, Mn, Fe, Cu, Co, and others),<sup>18,19</sup> polycyclic aromatic hydrocarbons (i.e., acenaphthene, anthracene, fluoranthene, and others),<sup>20,21</sup> and other carcinogens,<sup>22</sup> which exert a high potential health burden on cardiovascular, respiratory, and cancer diseases.<sup>23</sup> Therefore, understanding the magnitude and spatial and temporal distributions of FRD emissions is vital to better understand the interactions among FRD, air quality,

Received: January 31, 2019

Revised: May 7, 2019

Accepted: May 21, 2019

Published: May 22, 2019

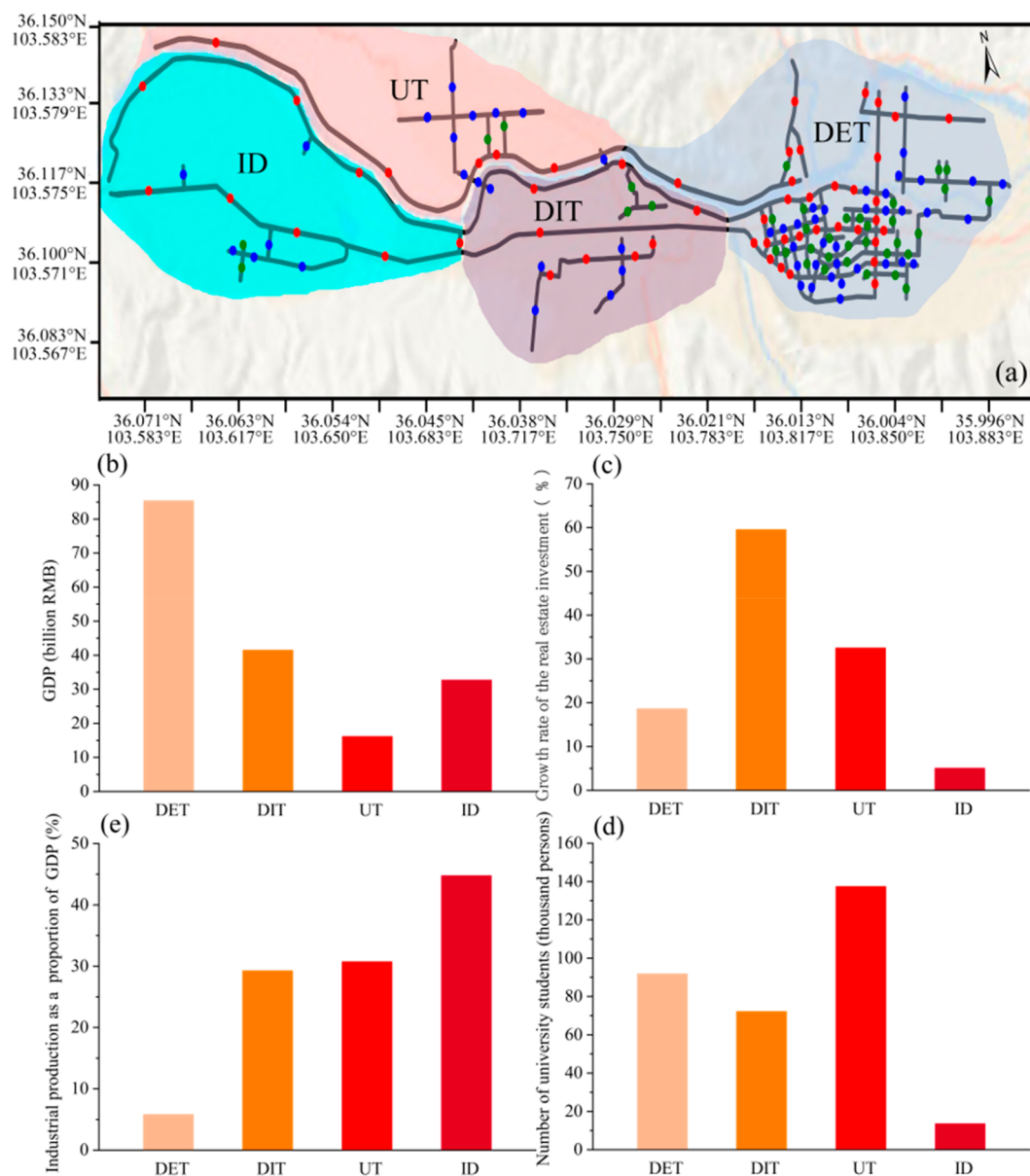


**Figure 1.** (a) Spatial distribution of sampling points in the study area (the red, blue, and green points represent the sampling points in the major roads, minor roads, and branch roads, respectively). And (b) GDP; (c) real estate investment growth rate; (d) number of university students (thousand persons); and (e) industrial production as a proportion of GDP in the four urban function zones (UFZs) of Lanzhou in 2017. DET = developed downtown; DIT = developing downtown; UT = university town; and ID = industrial district.

economic development, and public health. However, previous studies neglected or greatly underestimated FRD emissions,<sup>7</sup> resulting in high uncertainties in model estimates of PM concentrations, especially for PM<sub>2.5</sub>, and their environmental, health, and climatic effects.<sup>12,13,24,25</sup> For example, FRD emissions are not included in current Chinese emission inventories,<sup>26–29</sup> nor are they represented in many model simulations which use these inventories.<sup>30,31</sup>

FRD emissions are particularly important in developing urban areas due to the large amounts of vehicles, dust sources, and inhabitants. The urban environment can be separated into several distinctive urban function zones (UFZs) differentiated by the intensity of social/economic activities and the characteristics of environmental pollution,<sup>32–34</sup> such as downtown, residential, educational, and industrial zones.<sup>35</sup> In this study, we constructed a high-resolution (500 × 500 m<sup>2</sup>) gridded inventory for FRD PM<sub>2.5</sub> emissions in 2017 in the

urban area of Lanzhou, a major inland city in China threatened by the heavy FRD pollution. And we further characterized the spatial and temporal variability of emissions across different UFZs of Lanzhou and estimated their potential health impacts. Our results provided evidence to help plan and implement emission control measures of FRD in developing urban regions.

## EXPERIMENTAL SECTION

**Study Area.** Lanzhou, located in the center of mainland China (103.73°E, 36.03°N), is an important industrial city and transportation hub of northern China. Lanzhou has a unique river valley topography (Figure 1a), with high concentrations of PM in urban areas.<sup>36,37</sup> The urban area of Lanzhou is 1088 km<sup>2</sup>. The average annual temperature was 11.2 °C, and the annual precipitation was 341.3 mm in 2017.

**Table 1. Cumulative Particle Volume Percentages and Revised Values of  $k$  for Each Type of Road in the Four UFZs**

| UFZ <sup>a</sup> | type of road | particle volume percentage ( $\leq 2.5 \mu\text{m}$ ) | particle volume percentage ( $\leq 15 \mu\text{m}$ ) | revised $k$ ( $\text{g vkt}^{-1}$ ) |
|------------------|--------------|---|--|-------------------------------------|
| DET              | major roads  | 3.561   | 13.44  | 1.46                                |
|                  | minor roads  | 4.803   | 17.57  | 1.50                                |
|                  | branch roads | 3.651   | 14.16  | 1.42                                |
| DIT              | major roads  | 4.206   | 15.18  | 1.52                                |
|                  | minor roads  | 4.5   | 16.72  | 1.48                                |
|                  | branch roads | 3.199   | 12.33  | 1.43                                |
| UT               | major roads  | 3.6   | 15.53  | 1.27                                |
|                  | minor roads  | 4.505   | 16.63  | 1.49                                |
|                  | branch roads | 3.941   | 13.91  | 1.56                                |
| ID               | major roads  | 5.99  | 19.78  | 1.67                                |
|                  | minor roads  | 10.12   | 33.82  | 1.65                                |
|                  | branch roads | 8.874   | 31.82  | 1.53                                |

<sup>a</sup>Urban function zones: UFZs= urban function zones; DET = developed downtown; DIT = developing downtown; UT = university town; and ID = industrial district.

To characterize FRD emissions in different UFZs, we divided urban Lanzhou into four regions (Figure 1a). The developed downtown (DET) region, as the political, economic, and trade center of Lanzhou, is located in the east of the urban area and has the largest annual Gross Domestic Product (GDP) of \$14.6 billion among the four regions in 2017 (Figure 1b). The developing downtown (DIT) region, as a transport hub connected to each district, is located in the center of the urban area and has a rapidly increasing annual GDP of approximately \$6.7 billion in 2017. The real estate investment growth rate is 59.53%, indicating frequent demolition and construction activities (Figure 1b and c). The university town (UT), located in the northwest of urban area, has over 137 000 university students distributed among 17 universities and scores of primary and secondary schools. In the industrial district (ID), as a large petrochemical industrial base with several industrial factories, has a large share of industrial production in its annual GDP (44.76%). Coal and biomass burning are the dominant sources of anthropogenic aerosol emissions in the ID region.<sup>37,38</sup> Our sampling points cover the four divided regions above, including 45 main roads, 60 minor roads, and 55 branch roads (i.e., road segments between intersections) (Figure 1a).

**Revised AP-42 Method.** There exist a few methods to quantify FRD emissions based on different hypotheses and measurements, including the AP-42 method,<sup>39</sup> Testing Re-entrained Aerosol Kinetic Emissions from Roads (TRAKER) method and upwind-downwind method.<sup>40-42</sup> Our calculation was based on AP-42 but with updated parameters.

Especially, AP-42 was published in 1968 and has been gradually updated by the United States Environmental Protection Agency (USEPA). The method can be implemented with a standard sampling procedure suitable for constructing FRD emission inventories at a large scale. The FRD  $\text{PM}_{2.5}$  emission factor (EF,  $\text{g vkt}^{-1}$ , where vkt represents the number of vehicle kilometers traveled) on each paved road is calculated as follows:

$$EF = k \times \left(\frac{sL}{2}\right)^{0.65} \times \left(\frac{W}{3}\right)^{1.5} \quad (1)$$

where  $k$  is a particle size multiplier for  $\text{PM}_{2.5}$  smaller than  $i \mu\text{m}$  (unit:  $\text{g vkt}^{-1}$ );  $sL$  is the silt loading, which is defined as the amount of PM less than  $75 \mu\text{m}$  on the road surface per unit area (unit:  $\text{g m}^{-2}$ ); and  $W$  is the average vehicle weight (unit:

tons). The values of  $sL$  and  $W$  were obtained from our actual sampling in Lanzhou.

In this study, we divided the study domain into the grid of 1450 square cells ( $500 \times 500 \text{ m}^2$ ). Aggregated FRD  $\text{PM}_{2.5}$  emissions ( $E$ ,  $\text{g d}^{-1}$ ) from paved roads are calculated as follows:

$$E = \left(1 - \frac{P}{4N}\right) \times \sum_{i,j=1}^n EF_{i,j} \times F_{i,j} \times L_{i,j} \quad (2)$$

where  $P$  is the number of days (unit: days) when the daily precipitation exceeds 0.254 mm during the study period, which was taken from National Oceanic and Atmospheric Administration (NOAA)-National Climatic Data Center Surface (NCDC) (<ftp://ftp.ncdc.noaa.gov/pub/data/gsod/>);  $N$  is the study period (unit: days);  $F$  is the traffic volume on road  $i$  in grid cell  $j$  provided by the Traffic Police Detachment of the Public Security Bureau in Lanzhou (unit: vehicle  $\text{h}^{-1}$ ); and  $L$  is the length of road  $i$  in grid cell  $j$  (unit: km) obtained from the Open Street Map (<https://www.openstreetmap.org/#map=12/36.0781/103.7880>).

The particle size multiplier ( $k$ ) is a function of particle size. The default values of  $k$  were conducted based on sampling in the U.S.A. Moreover, the differences are also attributed to different method of estimating FRD emission factor. Therefore, the default value of  $k$  in AP-42 could lead to large uncertainties on the quantities of the FRD  $\text{PM}_{2.5}$  emissions in developing regions (such as Lanzhou). We revised the values of  $k$  based on sampling in Lanzhou as follows:

$$k = \frac{l_{2.5}}{l_{15}} \times k_{15} \quad (3)$$

where  $l$  is the mass percentage of particle mass with aerodynamic diameter less than 2.5 and 15  $\mu\text{m}$ ,  $k_{15}$  is the recommended value from AP-42 guidance document for 5.5  $\text{g vkt}^{-1}$ . The results are shown in Table 1.

**Estimate of Premature Mortality Rate.** We further simulated the FRD  $\text{PM}_{2.5}$  concentrations based on the Weather Research and Forecasting model coupled with Chemistry (WRF-Chem) Model and further estimated their health impacts by a pollution-exposure model.

The traditional epidemiological relation approach has been unanimously recognized and widely used to estimate the premature mortality rate attributable to  $\text{PM}_{2.5}$  exposure with respect to the international trade, residential, industrial,

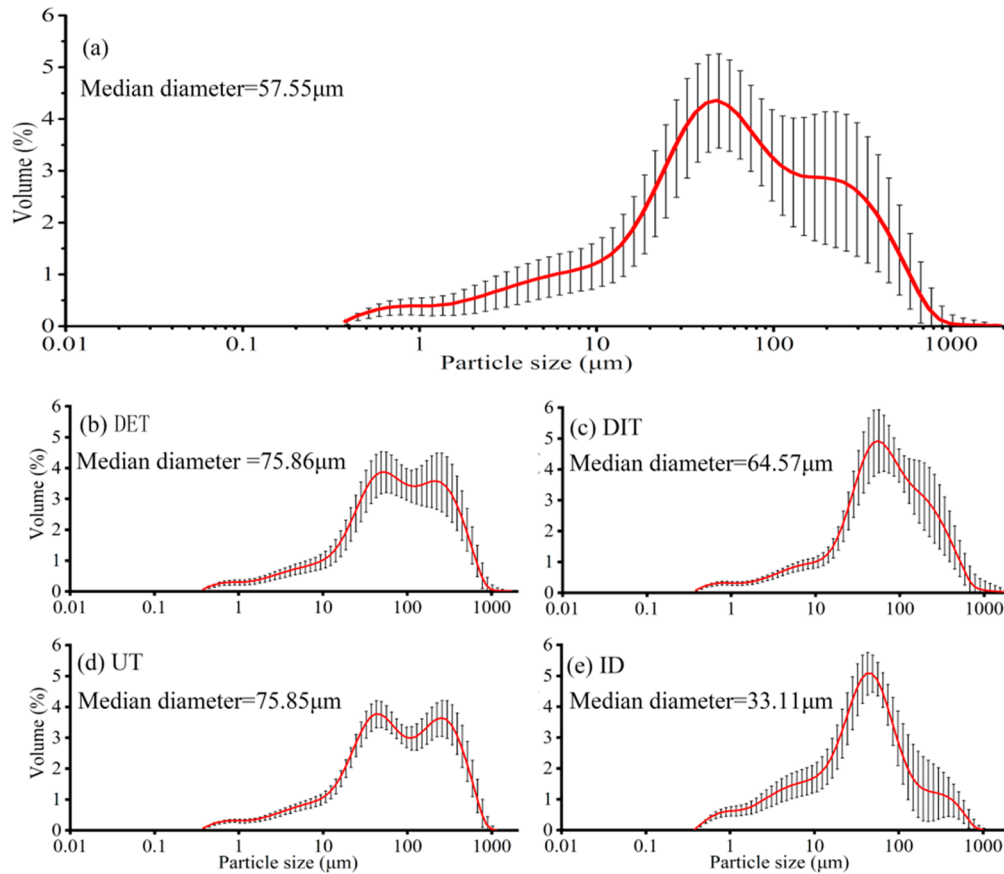


**Figure 2.** Average size distributions of road-deposited sediment in the study area (Figure 3a) and in the four UFZs including DET (Figure 3b), DIT (Figure 3c), UT (Figure 3d), and ID (Figure 3e). The error bar represents one standard deviation.

transportation and energy sectors.<sup>43–45</sup> In this study, we calculated the premature mortality burden ( $M$ , deaths  $y^{-1}$ ) attributable to FRD  $PM_{2.5}$  for chronic obstructive pulmonary disease (COPD), lung cancer (LC), ischemic heart disease (IHD), cerebrovascular disease (stroke), and acute lower respiratory infections (ALRI) through eq 4:

$$\sum_{i,j=1}^N M_{i,j} = \sum_{i,j=1}^N IM_{i,j} \times \sum_{i,j=1}^N P_i \quad (4)$$

where  $P$  is the population in UFZ  $i$ ; and  $IM$  is the incidence mortality of the disease  $j$  in UFZ  $i$  attributable to exposure to FRD  $PM_{2.5}$  (unit: deaths  $10^{-5}$  population  $y^{-1}$ ) calculated as follows:

$$\sum_{i,j=1}^N IM_{i,j} = \sum_{j=1}^N Y_j \times \frac{\sum_{i,j=1}^N RR_{i,j} - 1}{\sum_{i,j=1}^N RR_{i,j}} \quad (5)$$

$Y$  is the baseline mortality for disease type  $j$  (unit: deaths  $10^{-5}$  population  $y^{-1}$ );<sup>44</sup>  $RR$  is the relative risk for the disease  $j$  in UFZ  $i$ , which is estimated by the integrated exposure–response (IER) function:<sup>22</sup>

$$RR(C) = \begin{cases} 1 + \alpha[1 - \exp(-\gamma(C - C_0)^\delta)] & \text{for } C > C_0 \\ 1 & \text{for } C \leq C_0 \end{cases} \quad (6)$$

where  $C$  is the simulated FRD  $PM_{2.5}$  concentrations based on the WRF-Chem model (see Table S2 of the Supporting

Information, SI);  $C_0$  represents the theoretical minimum risk exposure level,  $\alpha$ ,  $\gamma$ , and  $\delta$  are parameters specific to disease  $j$ .<sup>45</sup> The key parameters for calculations of premature mortality have shown in Table S3.

## RESULTS

**Size Distribution of Road-Deposited Sediment.** The particle size of road-deposited sediment is critical to the assessment of FRD emissions and associated pollutant concentrations.<sup>18</sup> For urban Lanzhou as a whole, the particle volume distribution of road-deposited sediment showed the bimodal pattern, where the first peak was more dominant than the second peak. The first mode peaked at 40–79  $\mu\text{m}$ , and the second mode peaked at 159–316  $\mu\text{m}$  (Figure 2a). The size distributions of road dust deposited in the four UFZs differed significantly (Figure 2b–e). The percentage contributions of particles smaller than 100  $\mu\text{m}$  to the total road-deposited sediment were ordered as follows: ID (83.8%) > UT (65.0%) > DET (57.3%) > DIT (57.2%). The size distributions in the DET and UT both showed a bimodal pattern, with a large median size of 76  $\mu\text{m}$ . In the ID and DIT, the road-deposited sediment samples had unimodal distributions with small median sizes ranging from 33 to 65  $\mu\text{m}$ , because of a large amount of fly ash emitted from coal-fired factories and demolition and construction activities that greatly increase the proportion of fine particles.<sup>48</sup>

**Silt Loading.** The silt loading in the four UFZs decreased in the following order: DIT (0.62  $\text{g m}^{-2}$ ) > ID (0.44  $\text{g m}^{-2}$ ) > UT (0.34  $\text{g m}^{-2}$ ) > DET (0.28  $\text{g m}^{-2}$ ). These values were

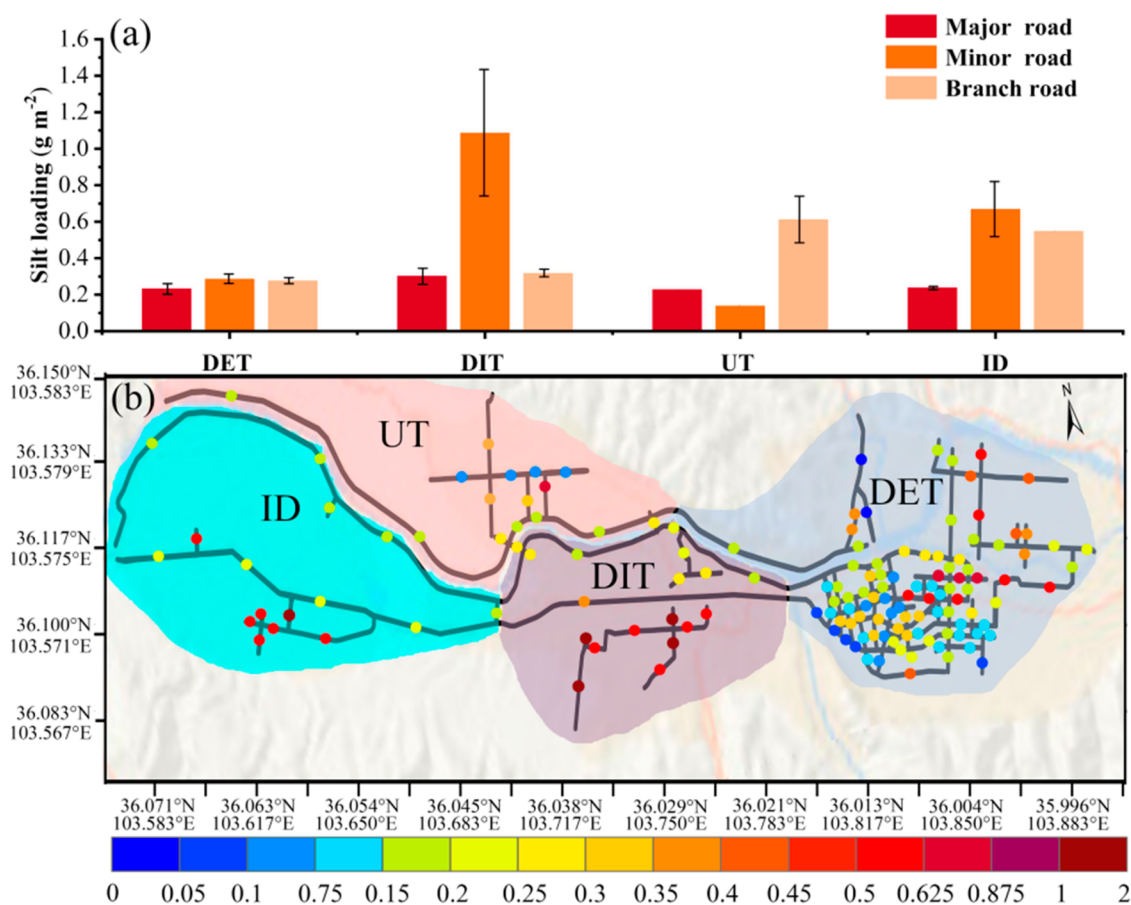


**Figure 3.** (a) Silt loading on three types of roads in each of the four UFZs (unit:  $\text{g m}^{-2}$ ; the error bar represents one standard deviation). (b) Spatial distribution of silt loading on sampling sites (unit:  $\text{g m}^{-2}$ ).

averaged over major, minor, and branch roads. Among the types of roads and UFZs, the highest value of silt loading,  $1.1 \pm 0.34 \text{ g m}^{-2}$ , occurred in the minor roads of the DIT, which was almost 4 times higher than that in the DET ( $0.3 \pm 0.02 \text{ g m}^{-2}$ ) with frequent street sweeping ( $3\text{--}4 \text{ times day}^{-1}$ ). This highest value was in the DIT because of frequent construction, seldom sweeping, and thus high proportion of bare soil on the roads (Figure 3a). The UT had the fewest population and relatively few human activities, where the value of silt loading was small on major and minor roads and high on branch roads, with average values of 0.24, 0.15, and  $0.62 \text{ g m}^{-2}$ , respectively (Figure 3b). The ID had relatively high silt loading values of approximately  $0.4 \text{ g m}^{-2}$  on minor and branch roads due to the mud carried by vehicles. Averaged over all UFZs, the amount of the silt loading for the three types of road were ordered as follows: minor roads ( $0.54 \text{ g m}^{-2}$ ) > branch roads ( $0.33 \text{ g m}^{-2}$ ) > major roads ( $0.29 \text{ g m}^{-2}$ ).

**Traffic Conditions.** Lanzhou has about 0.9 million vehicles in 2017, and the resulting traffic intensity highly affects FRD emissions. Among the four UFZs, the DET had the highest traffic volume, with more than 34 000 vehicles  $\text{day}^{-1}$  on major roads and 10 000 vehicles  $\text{day}^{-1}$  on minor and branch roads together. The DIT, with the second highest traffic volume, supported more than 30 000 vehicles  $\text{day}^{-1}$  on major roads. The traffic volumes in the UT and ID ranging from 2500 to 32 500 vehicles  $\text{day}^{-1}$  were lower than that the DET traffic volume (Figure 4a and b).

Traffic volumes had an apparent diurnal cycle, with a minimum value in the nighttime, a rapid increase after 7:00,

and a more gradual decrease after 23:00 local time (LT = UTC + 8 h). The traffic volumes ranging from 600 to 1500 vehicles  $\text{h}^{-1}$ , are remained stable and high in the daytime, attributable to traffic congestion in urban areas caused by an imperfect transportation infrastructure. Further contrasting data in weekdays and in weekends shows that the high-traffic periods are delayed by approximately one to 2 h on weekends compared with those on weekdays.

**FRD PM<sub>2.5</sub> Emissions.** The daily FRD PM<sub>2.5</sub> emission inventory in Lanzhou was constructed with high-resolution ( $500 \times 500 \text{ m}^2$ ) as shown in Figure 5a. Due to highly dense road networks and high silt loadings, a few locations in the central DET and eastern DIT have the highest FRD PM<sub>2.5</sub> emissions between  $3 \times 10^4$  and  $6 \times 10^4 \mu\text{g m}^{-2} \text{ d}^{-1}$ . Relatively low FRD PM<sub>2.5</sub> emissions ( $0.2 \times 10^4 \sim 1.2 \times 10^4 \mu\text{g m}^{-2} \text{ d}^{-1}$ ) occurred in the UT and ID zones (Figure 5a). The anthropogenic PM<sub>2.5</sub> emission fluxes were  $7.2 \times 10^4$ ,  $5.7 \times 10^4$ ,  $0.5 \times 10^4$ , and  $4.1 \times 10^4 \mu\text{g m}^{-2} \text{ d}^{-1}$  in the DET, DIT, UT, and ID, respectively, based on the PKU PM<sub>2.5</sub> inventory.<sup>38</sup> The value of PM<sub>2.5</sub> emissions from FRD was about two-fifths of that from combustion and industrial process sources in DET and DIT. Overall, the total FRD emission in urban Lanzhou was  $1141 \pm 71 \text{ kg d}^{-1}$ . The road dust accounted for 24.6% of urban PM<sub>2.5</sub> emissions (Figure 6a). Especially, the contributions of road dust to PM<sub>2.5</sub> emissions varied widely among four UFZs, ranging from 16.2% to 51.7% (Figure 6c–f). The magnitude of FRD PM<sub>2.5</sub> emissions in the four UFZs decreased in the following order: DET ( $415 \pm 31 \text{ kg d}^{-1}$ ) > DIT ( $367 \pm 43 \text{ kg$

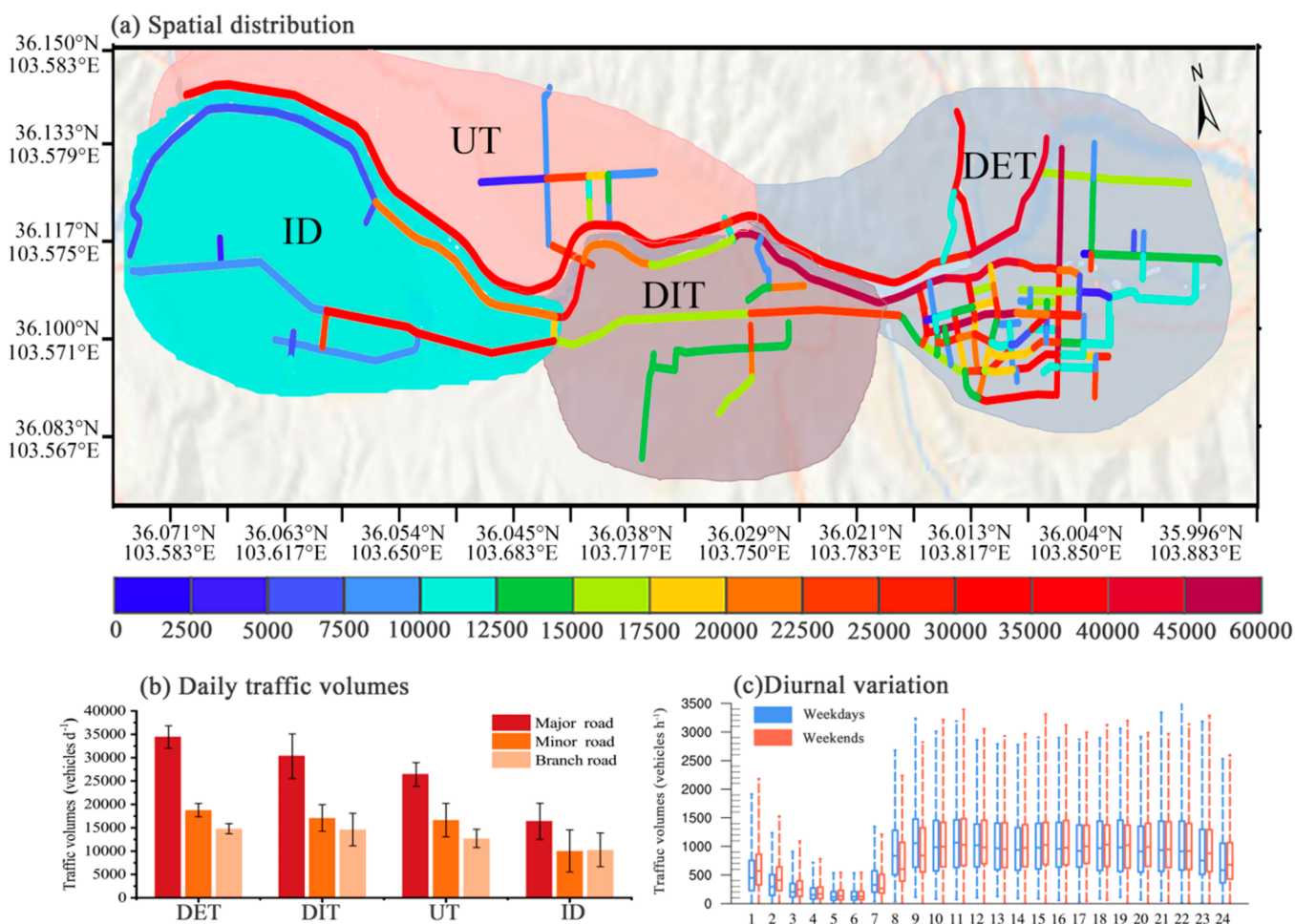


**Figure 4.** (a) Spatial distribution of daily traffic volume in Lanzhou (unit: vehicles  $d^{-1}$ ); (b) average daily traffic volumes on three level roads in each UFZ; (c) diurnal cycle of traffic volume (unit: vehicles  $h^{-1}$ ) on weekdays and weekends (dashes in the boxes denote the median traffic volumes; the lower and upper parts of the boxes represent the 25<sup>th</sup> and 75<sup>th</sup> percentiles for each data set, respectively. The dotted lines extending from the boxes indicate the maximum and minimum values).

$d^{-1}$ ) > ID ( $250 \pm 62 \text{ kg } d^{-1}$ ) > UT ( $109 \pm 13 \text{ kg } d^{-1}$ ) (Figure 5b).

The diurnal cycle of total FRD  $PM_{2.5}$  emissions mainly follows the variations in traffic volume. Summed over urban Lanzhou, the lowest hourly emission with value of  $7.11 \text{ kg } h^{-1}$  occurred at 5:00 LT in urban Lanzhou, after which emissions rose dramatically to  $58.63 \text{ kg } h^{-1}$  at 11:00 LT. Emissions remained high from 8:00 to 23:00 LT, a period with intensive human activities (Figure 5d). Meteorological condition, especially precipitation, dominates the seasonal variation of FRD  $PM_{2.5}$  emissions for urban Lanzhou (Figure 5c). Summed over urban Lanzhou, the monthly average FRD  $PM_{2.5}$  emission was the highest in winter ( $3.1 \times 10^4 \text{ kg month}^{-1}$ ), followed by spring and autumn (both  $2.8 \times 10^4 \text{ kg month}^{-1}$ ) and summer ( $2.7 \times 10^4 \text{ kg month}^{-1}$ ). The monthly variations of  $PM_{2.5}$  concentration at Lanzhou from observation and WRF-Chem model were shown in Figure 6b. Overall, the WRF-Chem model without FRD reproduced the temporal variation of  $PM_{2.5}$  well but always underestimated the observed  $PM_{2.5}$  concentrations of approximately  $20 \mu\text{g } m^{-3}$ . The temporal variation of simulated  $PM_{2.5}$  concentrations including FRD emissions are more consistent with that of observations especially in winter. However, the simulations always underestimated the observed  $PM_{2.5}$  concentrations in spring due to

not covering all of the natural dust source regions in the simulated domain.

**Estimate of Premature Mortality Rate Induced by FRD  $PM_{2.5}$  Exposure.** The premature mortality rate due to exposure to FRD  $PM_{2.5}$  is estimated at 30.2 premature deaths  $10^{-5}$  population  $y^{-1}$  in urban Lanzhou in 2017 (Confidence interval (CI) 95%: 27.4; 33.3), that is, 234.5 premature deaths for the total population of 2.5 million in urban Lanzhou. Of these deaths, 13.9% is related to COPD mortality, 9.7% to LC, 21.5% to ALRI, 31.8% to IHD, and 23.1% to stroke. The variation in the premature mortality rates for each disease is attributed to the difference in baseline mortality. In Lanzhou, IHD and stroke account for the most deaths, with values reaching 9.6 (CI 95%: 9.0; 10.1) and 6.9 (CI 95%: 6.4; 7.9) deaths  $10^{-5}$  population  $y^{-1}$ , respectively (Figure 7a). The estimated mortality rate from FRD  $PM_{2.5}$  varied substantially among the four UFZs, with relatively small values of 3.8 premature deaths  $10^{-5}$  population  $y^{-1}$  in the ID (Figure 7b). Owing to the interaction of a larger population, higher baseline mortality, higher emission, the premature mortality burden was obviously large in the DET and the DIT with high value of 157.1 and 44.9 premature deaths, respectively (Figure 7c).

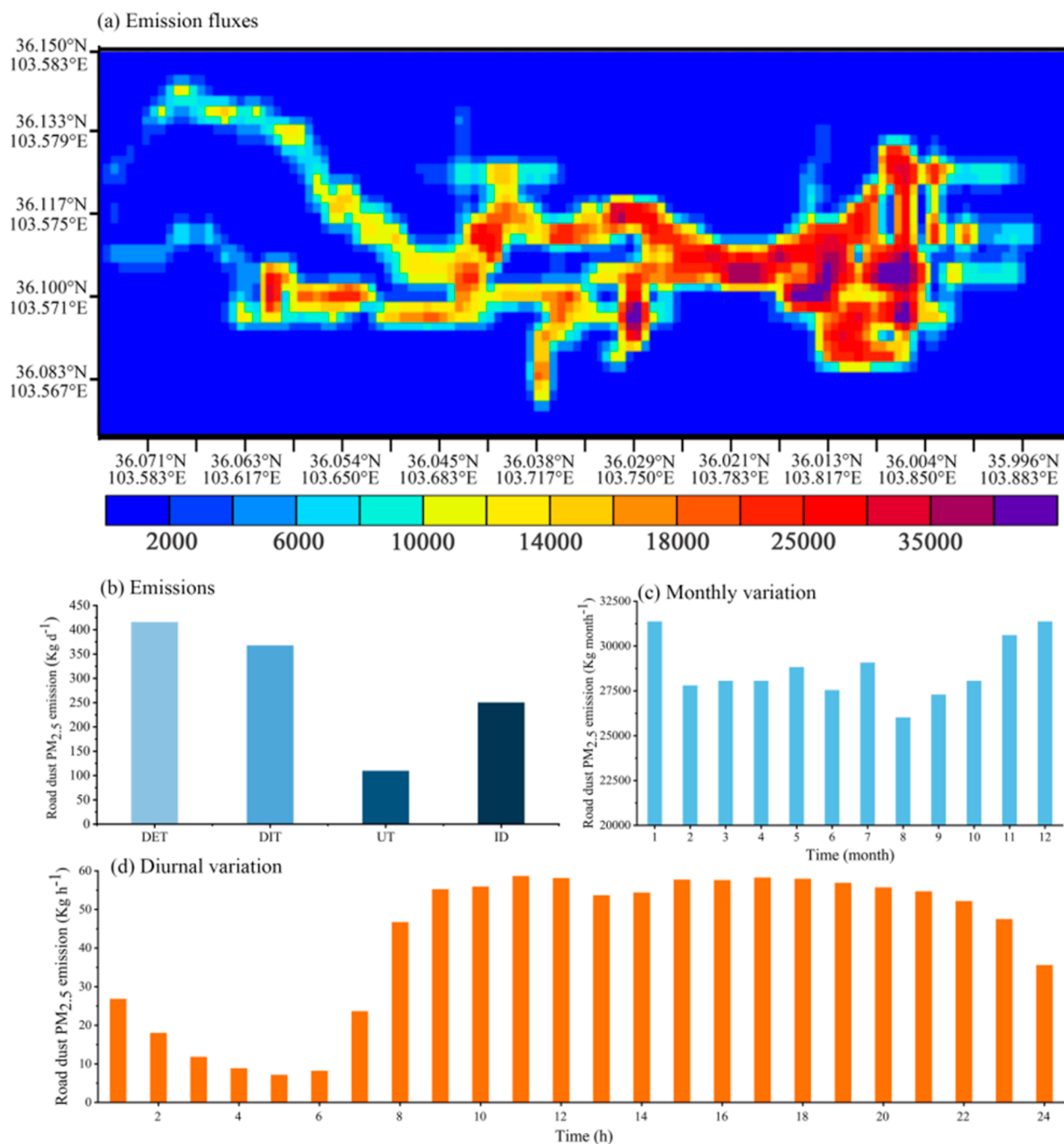


**Figure 5.** (a) Road dust  $PM_{2.5}$  emission fluxes (unit:  $\mu\text{g m}^{-2} \text{d}^{-1}$ ); (b) the total amounts of road dust  $PM_{2.5}$  emission in the four UFZs (unit:  $\text{kg d}^{-1}$ ); (c) monthly variations (unit:  $\text{kg month}^{-1}$ ); and (d) diurnal variations (unit:  $\text{kg h}^{-1}$ ) of road dust  $PM_{2.5}$  emissions.

## DISCUSSION

In the process of urbanization, a large (sometimes the largest) fraction of urban  $PM_{2.5}$  comes from FRD, which cause ambient air quality degradation and acute damage to public health.<sup>15–17,23</sup> UFZs, which are closely related to daily urban activities, are associated with distinctive characteristics of road-deposited sediment and FRD  $PM_{2.5}$  emissions.<sup>18,35</sup> We constructed a high-resolution gridded FRD  $PM_{2.5}$  emission inventory based on a revised AP-42 method<sup>39</sup> to investigate the characteristics of FRD  $PM_{2.5}$  emissions in the four UFZs and their mortality impacts through a traditional epidemiological relation approach<sup>44–48</sup> in the study.

The road-deposited sediment in Lanzhou predominantly comprises smaller particles ( $<100 \mu\text{m}$ , 57–84%), which can be easily released into atmosphere.<sup>18</sup> In particular, the road dust particles deposited in the ID region are much smaller than those deposited in other regions, with a median size of  $33.11 \mu\text{m}$ , because of a large amount of deposited fine particles originating from coal-fired factories and demolition and construction activities.<sup>37,38</sup> Thus, these particles could be suspended in the ambient atmosphere over a longer period, contain more heavy metal contents, and be more harmful to human health in the ID region than in the other regions.<sup>18,49</sup> Silt loading values are highly related to anthropogenic activities, e.g., frequent street sweeping reduces the silt

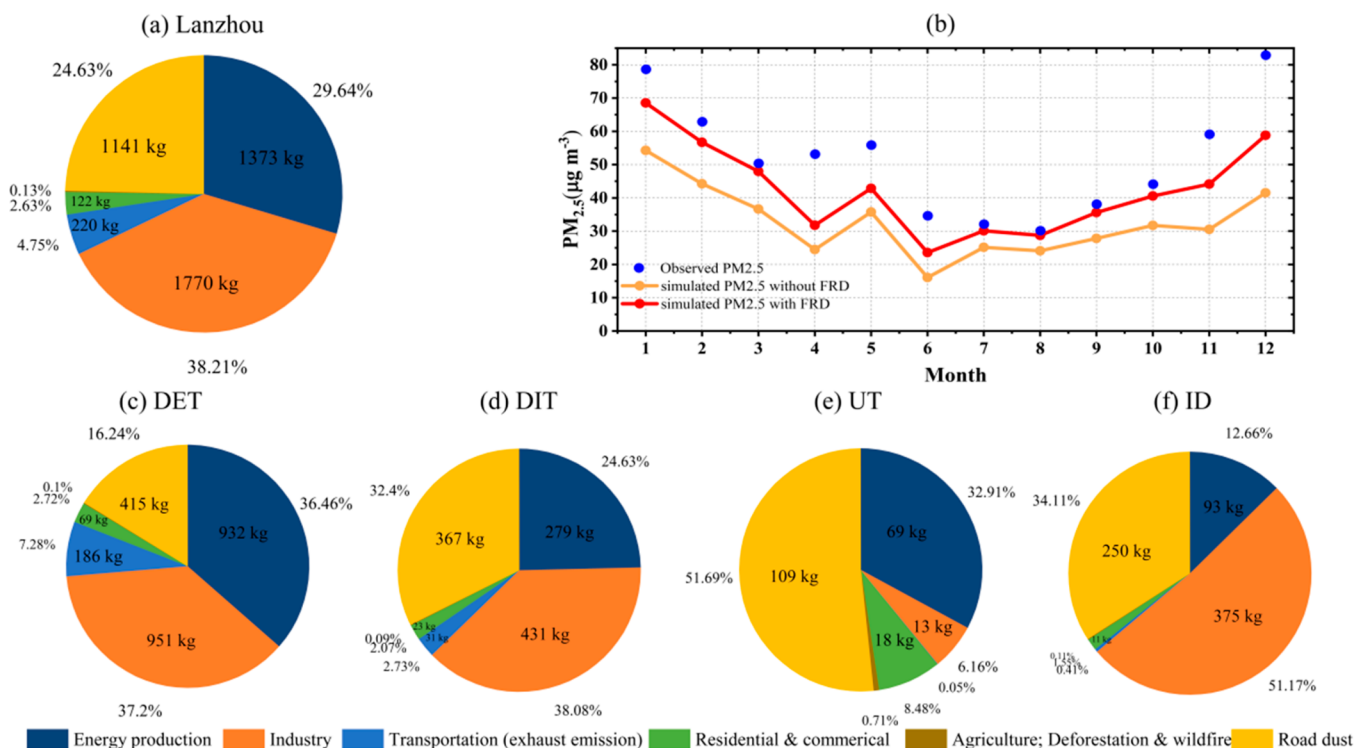


**Figure 6.** Source profiles for total emissions of PM<sub>2.5</sub> in (a) Lanzhou, (c) DET, (d) DIT, (e) UT, and (f) ID. And (b) monthly variations of PM<sub>2.5</sub> concentration (unit:  $\mu\text{g m}^{-3}$ ) from observation (blue dots), simulation without FRD (yellow line), and with FRD (red line) during 2017.

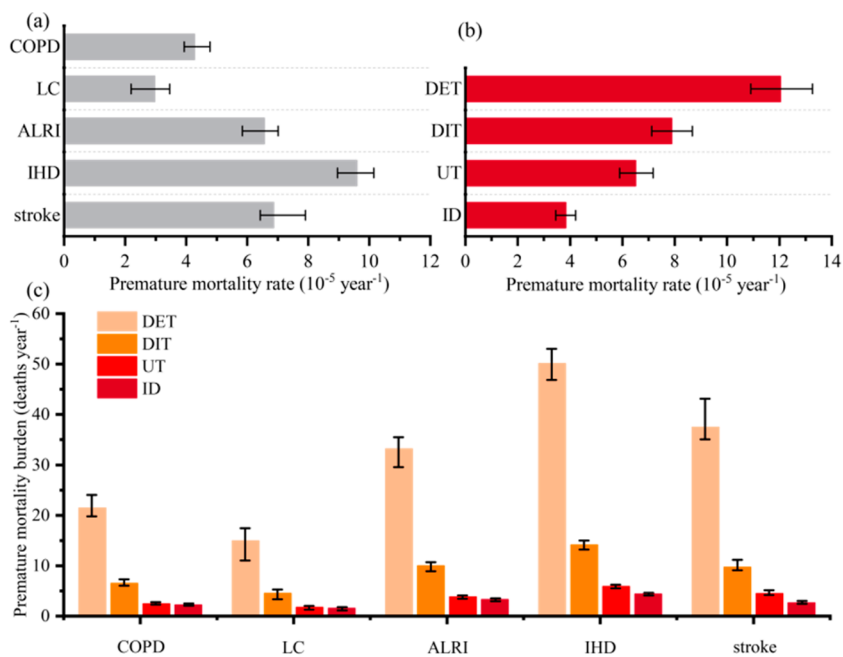


**Figure 7.** (a) Premature mortality rates in 2017 associated with FRD PM<sub>2.5</sub> exposure for chronic obstructive pulmonary disease (COPD), lung cancer (LC), acute lower respiratory infections (ALRI), ischemic heart disease (IHD), and cerebrovascular disease (stroke). (b) Premature mortality rates in the four UFZs. And (c) premature mortality burden in 2017 associated with FRD PM<sub>2.5</sub> exposure. The error bar denotes the 95% confidence intervals.

loadings, but transportation and construction activities lead to 2–10 times increases in silt loading.

The characteristics of FRD PM<sub>2.5</sub> emissions varied substantially among different UFZs. The FRD PM<sub>2.5</sub> emission is an one of main contributor to urban PM<sub>2.5</sub> emissions, accounting for 16.2% to 51.7% of the PM<sub>2.5</sub> emission among four UFZs. The total FRD PM<sub>2.5</sub> emission in the study area

was approximately 1141 kg d<sup>-1</sup>. The FRD PM<sub>2.5</sub> emission in the DET ranked the highest (415.35 kg d<sup>-1</sup>) due to the largest traffic volume, despite the frequent street sweeping. The DIT, ranked second (367.27 kg d<sup>-1</sup>), has the largest emission factor mainly due to the intensive construction activities. The spatial distribution of FRD PM<sub>2.5</sub> emissions demonstrates a significant relationship between FRD PM<sub>2.5</sub> emissions and human

activities: high emissions with values over  $3 \times 10^4 \mu\text{g m}^{-2} \text{d}^{-1}$  are mainly concurrent with relatively infrequent street sweeping, frequent construction activities, and high density of road networks. Compared with observation, the WRF-Chem model with FRD reproduced the monthly variation of  $\text{PM}_{2.5}$  better than that without FRD. It is noted that the revised AP-42 method used here only accounts for a limited number of factors including particle size of FRD, silt loading, vehicle weight, and precipitation. However, the previous studies pointed out that road characteristics (e.g., vehicle speed, types of vehicles, location, and topography),<sup>50</sup> other human activities (street cleaning activities and policies), and meteorological conditions (e.g., temperature, wind direction and wind speed, and relative humidity) also play important roles in FRD emissions.<sup>51</sup> The AP-42 method should be improved by including more factors in the future.

The estimated premature mortality rate induced by FRD  $\text{PM}_{2.5}$  exposure based on the traditional epidemiological relation approach was 234.5 (CI 95%: 212.2; 258.3) premature deaths in urban Lanzhou in 2017. Mortality due to FRD  $\text{PM}_{2.5}$  varied substantially among four UFZs. Compared to mortality from the other UFZs, premature deaths rates were the largest in the DET with value of 12.0 (CI 95%: 10.9; 13.2) premature deaths  $10^{-5}$  population  $\text{y}^{-1}$  owing to higher baseline mortality and larger dust emission. Note that the estimation of premature mortality induced by FRD exposure in the study may be underestimated due to ignoring the influence of the size distribution of particles, heavy metals, and polycyclic aromatic hydrocarbon.<sup>18,49,52</sup>

As emission reduction measures are being implemented rapidly for fossil fuel burning, vehicle exhaust, and the power sector, FRD  $\text{PM}_{2.5}$  emissions may represent a larger proportion of air pollution.<sup>7</sup> FRD PM emissions abatement could significantly improve urban air quality and protect public health.<sup>45</sup> Effective FRD  $\text{PM}_{2.5}$  mitigation measures may differ among the UFZs. Increasing the frequencies of street sweeping could reduce FRD  $\text{PM}_{2.5}$  emissions in the DIT, in combination with dust control measures for construction activities.<sup>51</sup> Moreover, use of dust suppressants with high hygroscopic and deliquescent properties is an effective mitigation measure in the DIT and ID, which areas have high silt loading and smaller particles.<sup>19</sup> Moreover, the utilization of emission control technologies of factories should be promoted in the long run, such as implementing retirement of small and low-efficient power plants and applying end-of-pipe controls,<sup>53,54</sup> to fundamentally reduce fine particles in FRD in the ID.

## ■ ASSOCIATED CONTENT

### 📄 Supporting Information

The Supporting Information is available free of charge on the ACS Publications website at DOI: 10.1021/acs.est.9b00666.

Details of road dust sampling and measuring characteristics of road-deposited sediment (Text S1; Figure S1); simulation of FRD  $\text{PM}_{2.5}$  concentrations based on the WRF-Chem model (Text S2; Table S1, S2; Figure S4); source of ground monitoring  $\text{PM}_{2.5}$  data (Text S3); the diurnal cycle of traffic volume in three types of roads (Text S3, Figure S2); and the characteristics of FRD  $\text{PM}_{10}$  emission (Text S4, Figure S3) (PDF)

## ■ AUTHOR INFORMATION

### Corresponding Author

\*Phone/fax: 0931-8914139; e-mail: [hjp@lzu.edu.cn](mailto:hjp@lzu.edu.cn).

### ORCID

Siyu Chen: 0000-0003-2532-6050

### Notes

The authors declare no competing financial interest.

## ■ ACKNOWLEDGMENTS

This research was supported by the Foundation for National Natural Science Foundation of China (No. 91837103, No. 41775003) and the Foundation of Key Laboratory for Semi-Arid Climate Change of the Ministry of Education in Lanzhou University.

## ■ REFERENCES

- (1) van Donkelaar, A.; Martin, R. V.; Brauer, M.; Boys, B. L. Use of satellite observations for long-term exposure assessment of global concentrations of fine particulate matter. *Environ. Health Perspect.* **2015**, *123*, 135–143 Oct 24, 2014. .
- (2) Cohen, A.; Brauer, M.; Burnett, R.; Anderson, H.; Frostad, J.; Estep, K.; Balakrishnan, K.; Brunekreef, B.; Dandona, L.; Dandona, R.; Feigin, V.; Freedman, G.; Hubbell, B.; Jobling, A.; Kan, H.; Knibbs, L.; Liu, Y.; Martin, R.; Morawska, L.; Pope, A.; Shin, H.; Straif, K.; Shaddick, G.; Thomas, M.; van Dingenen, R.; van Donkelaar, A.; Vos, T.; Murray, C.; Forouzanfar, M. Estimates and 25-year trends of the global burden of disease attributable to ambient air pollution: an analysis of data from the Global Burden of Diseases Study 2015. *Lancet* **2017**, *389*, 1907–1918.
- (3) Chowdhury, S.; Dey, S. Cause-specific premature death from ambient  $\text{PM}_{2.5}$  exposure in India: Estimate adjusted for baseline mortality. *Environ. Int.* **2016**, *91*, 283–290.
- (4) Han, X.; Liu, Y.; Gao, H.; Ma, J.; Mao, X.; Wang, Y.; Ma, X. Forecasting  $\text{PM}_{2.5}$  induced male lung cancer morbidity in China using satellite retrieved  $\text{PM}_{2.5}$  and spatial analysis. *Sci. Total Environ.* **2017**, *607–608*, 1009–1017.
- (5) Abu-Allaban, M.; Gillies, J.; Gertler, A.; Clayton, R.; Proffitt, D. Tailpipe, resuspended road dust, and brake-wear emission factors from on-road vehicles. *Atmos. Environ.* **2003**, *37*, S283–S293.
- (6) Kuhns, H.; Etyemezian, V.; Green, M.; Hendricson, K.; Gown, M.; Barton, K.; Pitchford, M. Vehicle-based road dust emission measurement: Effect of precipitation, winter-time road sanding and street sweepers on inferred  $\text{PM}_{10}$  emission potentials from paved and unpaved roads. *Atmos. Environ.* **2003**, *37* (32), 4573–4582.
- (7) Amato, F.; Alastuey, A.; de la Rosa, J.; Castanedo, Y. G.; de la Campa, A. S.; Pandolfi, M.; Lozano, A.; Gonzalez, J. C.; Querol, X. Trends of Road Dust Emissions Contributions on Ambient Air Particulate Levels at Rural, Urban and Industrial Sites in Southern Spain. *Atmos. Chem. Phys.* **2014**, *14* (7), 3533–3544.
- (8) Thorpe, A.; Harrison, R. Sources and properties of non-exhaust particulate matter from road traffic: a review. *Sci. Total Environ.* **2008**, *400* (1), 270–282.
- (9) Gunawardana, C.; Goonetilleke, A.; Egodawatta, P.; Dawes, L.; Kokot, S. Source characterisation of road dust based on chemical and mineralogical composition. *Chemosphere* **2012**, *87* (2), 163–170.
- (10) Han, L.; Zhou, W.; Li, W.; Li, L. Impact of urbanization level on urban air quality: A case of fine particles ( $\text{PM}_{2.5}$ ) in Chinese cities. *Environ. Pollut.* **2014**, *194*, 163–170.
- (11) Chan, C.; Yao, X. Air pollution in mega cities in China. *Atmos. Environ.* **2008**, *42*, 1–42.
- (12) Chen, S.; Jiang, N.; Huang, J.; Xv, X.; Zhang, H.; Zang, Z.; Huang, K.; Xu, X.; Wei, Y.; Guan, X.; Zhang, X.; Hu, Z.; Feng, T.; Luo, Y. Quantifying contributions of natural and anthropogenic dust emission from different climatic regions. *Atmos. Environ.* **2018**, *191*, 94–104.

- (13) Chen, S.; Jiang, N.; Huang, J.; Zang, Z.; Guan, X.; Ma, X.; Luo, Y.; Li, J.; Zhang, X.; Zhang, Y. Estimation of indirect and direct anthropogenic dust emission at the global scale. *Atmos. Environ.* **2019**, *200*, 50–60.
- (14) Huang, J.; Liu, J.; Chen, B.; Nasiri, S. Detection of anthropogenic dust using CALIPSO lidar measurements. *Atmos. Chem. Phys.* **2015**, *15* (20), 11653–11665.
- (15) Sahu, S.; Beig, G.; Parkhi, N. Emissions inventory of anthropogenic PM<sub>2.5</sub> and PM<sub>10</sub> in Delhi during Commonwealth Games 2010. *Atmos. Environ.* **2011**, *45* (34), 6180–6190.
- (16) Pereira, G.; Teinila, K.; Custodio, D.; Santos, A. G.; Xian, H.; Hillamo, R.; Alves, C.; de Andrade, J. B.; da Rocha, G. O.; Kumar, P.; Balasubramanian, R.; Andrade, M.; Vasconcellos, P. d. C. Particulate pollutants in the Brazilian city of São Paulo: 1-year investigation for the chemical composition and source apportionment. *Atmos. Chem. Phys.* **2017**, *17*, 11943–11969.
- (17) Amato, F.; Schaap, M.; Reche, C.; Querol, X. Road Traffic: A Major Source of Particulate Matter in Europe. *Hdb Env Chem.* **2013**, *26*, 165–194.
- (18) Zhao, H.; Li, X.; Wang, X. Heavy metal contents of road-deposited sediment along the urban–rural gradient around Beijing and its potential contribution to runoff pollution. *Environ. Sci. Technol.* **2011**, *45*, 7120–7127.
- (19) Amato, F.; Karanasiou, A.; Cordoba, p.; Alastuey, A.; Moreno, T.; Lucarelli, F.; Nava, S.; Calzolari, G.; Querol, X. Effects of Road Dust Suppressants on PM Levels in a Mediterranean Urban Area. *Environ. Sci. Technol.* **2014**, *48* (14), 8069–8077.
- (20) Gunawardena, J.; Egodawatta, P.; Ayoko, G.; Goonetilleke, A. Role of traffic in atmospheric accumulation of heavy metals and polycyclic aromatic hydrocarbons. *Atmos. Environ.* **2012**, *54*, 502–510.
- (21) Ma, Y.; Liu, A.; Egodawatta, P.; McGree, J.; Goonetilleke, A. Quantitative assessment of human health risk posed by polycyclic aromatic hydrocarbons in urban road dust. *Sci. Total Environ.* **2017**, *575*, 895–904.
- (22) Nagpure, A.; Gurjar, B.; Kumar, V.; Kumar, P. Estimation of exhaust and non-exhaust gaseous, particulate matter and air toxics emissions from on-road vehicles in Delhi. *Atmos. Environ.* **2016**, *127*, 118–124.
- (23) Burnett, R.; Pope, C.; Ezzati, M.; Olives, C.; Lim, S.; Mehta, S.; Shin, H.; Singh, G.; Hubbell, B.; Brauer, M.; Anderson, H.; Smith, K.; Balmes, J.; Bruce, N.; Kan, H.; Laden, F.; Pruss-Ustun, A.; Turner, M.; Gapstur, S.; Diver, W.; Cohen, A. Integrated Risk Function for Estimating the Global Burden of Disease Attributable to Ambient Fine Particulate Matter Exposure. *Environ. Health Perspect.* **2014**, *122* (4), 397–403.
- (24) Brunekreef, B.; Forsberg, B. Epidemiological evidence of effects of coarse airborne particles on health. *Eur. Respir. J.* **2005**, *26*, 309–318.
- (25) Huang, J.; Wang, T.; Wang, W.; Li, Z.; Yan, H. Climate effects of dust aerosols over East Asian arid and semiarid regions. *J. Geophys. Res.-Atmos.* **2014**, *119* (19), 11398–11416.
- (26) Zhang, Y.; Tao, S. Global atmospheric emission inventory of polycyclic aromatic hydrocarbons (PAHs) for 2004. *Atmos. Environ.* **2009**, *43* (4), 812–819.
- (27) Xu, S.; Liu, W.; Tao, S. Emission of polycyclic aromatic hydrocarbons in China. *Environ. Sci. Technol.* **2006**, *40* (3), 702–708.
- (28) Li, M.; Zhang, Q.; Kurokawa, J.; Woo, J.; He, K.; Lu, Z.; Ohara, T.; Song, Y.; Streets, D. G.; Carmichael, G. R.; Cheng, Y.; Hong, C.; Huo, H.; Jiang, X.; Kang, S.; Liu, F.; Su, H.; Zheng, B. MIX: a mosaic Asian anthropogenic emission inventory under the international collaboration framework of the MICS-Asia and HTAP. *Atmos. Chem. Phys.* **2017**, *17* (2), 935–963.
- (29) Lin, J.; Pan, D.; Davis, S. J.; Zhang, Q.; He, K.; Wang, C.; Streets, D. G.; Wuebbles, D. J.; Guan, D. China's international trade and air pollution in the United States. *Proc. Natl. Acad. Sci. U. S. A.* **2014**, *111* (5), 1736–1741.
- (30) Lin, J.; Tong, D.; Davis, S.; Ni, R.; Tan, X.; Pan, D.; Zhao, H.; Lu, Z.; Streets, D.; Feng, T.; Zhang, Q.; Yan, Y.; Hu, Y.; Li, J.; Liu, Z.; Jiang, X.; Geng, G.; He, K.; Huang, Y.; Guan, D. Global climate forcing of aerosols embodied in international trade. *Nat. Geosci.* **2016**, *9*, 790–794.
- (31) Liu, M.; Lin, J.; Wang, Y.; Sun, Y.; Zheng, B.; Shao, J.; Chen, L.; Zheng, Y.; Chen, J.; Fu, T.; Yan, Y.; Zhang, Q.; Wu, Z. Spatiotemporal variability of NO<sub>2</sub> and PM<sub>2.5</sub> over Eastern China: observational and model analyses with a novel statistical method. *Atmos. Chem. Phys.* **2018**, *18*, 12933–12952.
- (32) Harris, C. A Functional Classification of Cities in the United States. *Geogr. Rev.* **1943**, *33* (1), 86–99.
- (33) Lebel, L.; Garden, P.; Banaticla, M.; Lasco, R.; Contreras, A.; Mitra, A.; Sharma, C.; Nguyen, H.; Ooi, G.; Sari, A. Management into the Development Strategies of Urbanizing Regions in Asia: Implications of Urban Function, Form, and Role. *J. Ind. Ecol.* **2007**, *11* (2), 61–81.
- (34) Zhang, X.; Wang, J.; Wang, Y.; Liu, H.; Sun, J.; Zhang, Y. Changes in chemical components of aerosol particles in different haze regions in China from 2006 to 2013 and contribution of meteorological factors. *Atmos. Chem. Phys. Discuss.* **2015**, *15*, 19197–19238.
- (35) Yao, L.; Wei, W.; Yu, Y.; Xiao, X.; Chen, L. Rainfall-runoff risk characteristics of urban function zones in Beijing using the SCS-CN model. *J. Geogr. Sci.* **2018**, *28* (5), 656–668.
- (36) Jin, L.; Qiu, J.; Zhang, Y.; Qiu, W.; He, X.; Wang, Y.; Sun, Q.; Li, M.; Zhao, N.; Cui, H.; et al. Ambient air pollution and congenital heart defects in Lanzhou, China. *Environ. Res. Lett.* **2015**, *10* (7), 074005.
- (37) Wang, Y.; Jia, C.; Tao, J.; Zhang, L.; Liang, X.; Ma, J.; Gao, H.; Huang, T.; Zhang, K. Chemical characterization and source apportionment of PM 2.5 in a semi-arid and petrochemical-industrialized city, Northwest China. *Sci. Total Environ.* **2016**, *573*, 1031–1040.
- (38) Huang, Y.; Shen, H. Z.; Chen, H.; Wang, R.; Zhang, Y. Y.; Su, S.; Chen, Y. C.; Lin, N.; Zhuo, S. J.; Zhong, Q. R.; Wang, X. L.; Liu, J. F.; Li, B. G.; Liu, W. X.; Tao, S. Quantification of global primary emissions of pm2.5, pm10, and tsp from combustion and industrial process sources. *Environ. Sci. Technol.* **2014**, *48*, 13834–13843.
- (39) *Compilation of Air Pollutant EFs: Final Stationary Point and Area Sources, Miscellaneous Sources: Paved Roads Final Section*; United States Environmental Protection Agency, 2011; [www3.epa.gov/ttn/chief/ap42/ch13/final/c13s0201.pdf](http://www3.epa.gov/ttn/chief/ap42/ch13/final/c13s0201.pdf).
- (40) Kuhns, H.; Etyemezian, V.; Landwehr, D.; MacDougall, C.; Pitchford, M.; Green, M. Testing Re-entrained Aerosol Kinetic Emissions from Roads: a new approach to infer silt loading on roadways. *Atmos. Environ.* **2001**, *35* (16), 2815–2825.
- (41) Dyck, R.; Stukel, J. Fugitive dust emissions from trucks on unpaved roads. *Environ. Sci. Technol.* **1976**, *10* (10), 1046–1048.
- (42) Gillies, J. A.; Etyemezian, V.; Kuhns, H.; Nikolic, D.; Gillette, D. Effect of vehicle characteristics on unpaved road dust emissions. *Atmos. Environ.* **2005**, *39* (13), 2341–2347.
- (43) Zhang, Q.; Jiang, X.; Tong, D.; Davis, S.; Zhao, H.; Geng, G.; Feng, T.; Zheng, B.; Lu, Z.; Streets, D. G.; et al. Transboundary health impacts of transported global air pollution and international trade. *Nature* **2017**, *543* (7647), 705–709.
- (44) Upadhyay, A.; Dey, S.; Chowdhury, S.; Goyal, P. Expected health benefits from mitigation of emissions from major anthropogenic PM<sub>2.5</sub> sources in India: Statistics at state level. *Environ. Pollut.* **2018**, *242*, 1817–1826.
- (45) Chowdhury, S.; Dey, S. Cause-specific premature death from ambient PM<sub>2.5</sub> exposure in India: Estimate adjusted for baseline mortality. *Environ. Int.* **2016**, *91*, 283–290.
- (46) Lozano, R.; Naghavi, M.; Foreman, K.; Lim, S.; Shibuya, K.; Aboyans, V.; Abraham, J.; Adair, T.; Aggarwal, R.; Ahn, S.; et al. Global and regional mortality from 235 causes of death for 20 age groups in 1990 and 2010: a systematic analysis for the Global Burden of Disease Study 2010. *Lancet* **2012**, *380*, 2095–2128.
- (47) Apte, J.; Marshall, J.; Cohen, A.; Brauer, M. Addressing Global Mortality from Ambient PM<sub>2.5</sub>. *Environ. Sci. Technol.* **2015**, *49* (13), 8057–8066.

(48) Ta, W.; Wang, T.; Xiao, H.; Zhu, X.; Xiao, Z. Gaseous and particulate air pollution in the Lanzhou Valley, China. *Sci. Total Environ.* **2004**, *320* (2–3), 163–176.

(49) Philip, S.; Martin, R.; Snider, G.; Weagle, C.; van Donkelaar, A.; Brauer, M.; Henze, D.; Klimont, Z.; Venkataraman, C.; Guttikunda, S.; Zhang, Q. Anthropogenic fugitive, combustion and industrial dust is a significant, underrepresented fine particulate matter source in global atmospheric models. *Environ. Res. Lett.* **2017**, *12*, 044018.

(50) Etyemezian, V.; Kuhns, H.; Gillies, J.; Chow, J.; Hendrickson, K.; Gown, M.; Pitchford, M. Vehicle-based road dust emission measurement (III):effect of speed, traffic volume, location, and season on PM 10road dust emissions in the Treasure Valley, ID. *Atmos. Environ.* **2003**, *37* (32), 4583–4593.

(51) Amato, F.; Querol, X.; Johansson, C.; Nagl, C.; Alastuey, A. A review on the effectiveness of street sweeping, washing and dust suppressants asurban PM control methods. *Sci. Total Environ.* **2010**, *408* (16), 3070–3084.

(52) Zhang, Y.; Tao, S.; Shen, H.; Ma, J. Inhalation exposure to ambient polycyclic aromatic hydrocarbons and lung cancer risk of Chinese population. *Proc. Natl. Acad. Sci. U. S. A.* **2009**, *106* (50), 21063–21067.

(53) Cao, R.; Tan, H.; Xiong, Y.; Mikulčić, H.; Vujanović, M.; Wang, X.; Duić, N. Improving the Removal of Particles and Trace Elements from Coal-fired Power Plants by Combining a Wet Phase Transition Agglomerator with Wet Electrostatic Precipitator. *J. Cleaner Prod.* **2017**, *161*, 1459–1465.

(54) Tong, D.; Zhang, Q.; Liu, F.; Geng, G.; Zheng, Y.; Xue, T.; Hong, C.; Wu, R.; Qin, Y.; Zhao, H.; et al. Current emissions and future mitigation pathways of coal-fired power plants in China from 2010 to 2030. *Environ. Sci. Technol.* **2018**, *52* (21), 12905–12914.